

## Decay of the neutron-rich isotope $^{113}\text{Ru}$ to $^{113}\text{Rh}$

J. Kurpeta<sup>1,a</sup>, G. Lhersonneau<sup>2,b</sup>, A. Płochocki<sup>1</sup>, J.C. Wang<sup>2,c</sup>, P. Dendooven<sup>2,d</sup>, A. Honkanen<sup>2,e</sup>, M. Huhta<sup>2,f</sup>, M. Oinonen<sup>2,g</sup>, H. Penttilä<sup>2</sup>, K. Peräjärvi<sup>2,h</sup>, J.R. Persson<sup>2,i</sup>, and J. Äystö<sup>2,3</sup>

<sup>1</sup> Institute of Experimental Physics, Warsaw University, ul. Hoża 69, 00-681 Warszawa, Poland

<sup>2</sup> Department of Physics, University of Jyväskylä, P.O. Box. 35, FIN-40351, Jyväskylä, Finland

<sup>3</sup> EP-ISOLDE, CERN 23, CH-1211, Geneva, Switzerland

Received: 18 January 2001 / Revised version: 29 November 2001

Communicated by C. Signorini

**Abstract.** The decay of neutron-rich isotope  $^{113}\text{Ru}$  obtained as on-line mass separated product of proton-induced fission has been investigated by  $\gamma\gamma$  coincidence and spectrum multiscaling measurements. Decay schemes for both low- and high-spin isomers of  $^{113}\text{Ru}$  have been constructed. The level scheme of  $^{113}\text{Rh}$  is considerably extended. Systematics of the lowest-lying rhodium levels is smooth. The picture of shape coexistence established for neutron-rich Rh isotopes near-neutron midshell is confirmed with the observation of a  $K = 1/2$  deformed band, with its  $3/2^+$  state at 600 keV being the lowest-lying *level and of probable  $7/2^+$  and  $5/2^+$  band members*. A large fraction of  $\beta$  feeding is found to populate high-lying levels in  $^{113}\text{Rh}$ . The GT strength in  $^{113}\text{Ru}^m$  decay is significantly larger than for the decay of  $^{113}\text{Ru}_g$  and of lighter rhodium isotopes.

**PACS.** 27.60.+j  $90 \leq A \leq 149$  – 23.20.Lv Gamma transitions and level energies

### Introduction

Observation of new exotic activities and detailed investigations of the structure of their daughters provide stringent tests for nuclear models, in particular of their predictive power far from the regions where they have been designed originally. This is especially important with respect to the current efforts to build facilities for the production of very exotic nuclei. Preliminary results on the decay of  $^{113}\text{Tc}$ ,  $^{113}\text{Ru}$  and  $^{113}\text{Rh}$  were presented in [1]. Recently, we

have reported in a more detailed way on the new decay of  $^{113}\text{Tc}$  to  $^{113}\text{Ru}$  [2] and on its branch to  $^{112}\text{Ru}$  by  $\beta$ -delayed neutron emission [3]. In this work, we present extended data on the decay of the neutron-rich  $^{113}\text{Ru}$  isotope. This decay was unambiguously identified for the first time using on-line mass separation with the ion-guide technique by Penttilä *et al.* [4]. The decay scheme of  $^{113}\text{Ru}$  presented some inconsistencies, *e.g.*, comparable strong  $\beta$  feedings to states of very different spins, which usually results from limited nature of the experimental data. After the upgrade of the IGISOL facility at Jyväskylä [5, 6] yields of these nuclei have increased by typically two orders of magnitude. As a consequence of greater sensitivity, new  $\beta$  branches to high-lying levels have been observed for several decays in this region as, *e.g.*, of  $^{111}\text{Ru}$  to  $^{111}\text{Rh}$  [7] and  $^{112}\text{Rh}$  to  $^{112}\text{Pd}$  [8] which are close neighbours of the ones discussed here. Moreover, a new 0.5 s isomer has been identified in  $^{113}\text{Ru}$  [2], the decay of which towards high-spin levels in  $^{113}\text{Rh}$  makes a revision of the feedings necessary. These facts motivated the present study the main goal of which was to improve the  $^{113}\text{Ru}$  decay scheme.

The odd-proton ( $Z = 45$ ) rhodium isotopes are situated below the  $Z = 50$  major shell closure. Accordingly, the low-lying states have been interpreted by invoking the spherical  $p_{1/2}$  and  $g_{9/2}$  single-particle states with, in addition, a number of higher seniority ( $\nu$ ) levels. In particular, the  $7/2^+$  ground states have been discussed as cases of the  $I = j - 1$  anomaly based on a  $\nu = 3$  configuration

<sup>a</sup> e-mail: jkurpeta@mimuw.edu.pl

<sup>b</sup> Present address: INFN, Laboratori Nazionali di Legnaro, Via Romea 4, 35020 Legnaro, Italy.

<sup>c</sup> Present address: Argonne National Laboratory, 9700 South Cass Avenue, Argonne, IL 60439, USA.

<sup>d</sup> Present address: KVI, Zernikelaan 25, NL-9747 AA Groningen, The Netherlands.

<sup>e</sup> Present address: Helsinki Institute of Physics, P.O. Box 9, Siltavuorenpenger 20 C, 00014 University of Helsinki, Finland.

<sup>f</sup> Present address: Nokia, Tampere, Finland.

<sup>g</sup> Present address: EP-ISOLDE, CERN 23, CH-1211, Geneva, Switzerland and Helsinki Institute of Physics, P.O. Box 9, Siltavuorenpenger 20 C, 00014 University of Helsinki, Finland.

<sup>h</sup> Present address: EP-ISOLDE, CERN 23, CH-1211 Geneva, Switzerland.

<sup>i</sup> Present address: Department of Mathematics and Science, Högskolan Kristianstad, SE-291 88 Kristianstad, Sweden.

following ref. [9]. Another interesting feature of rhodium isotopes is the presence of a  $K = 1/2$  band at rather low energy, especially near the neutron midshell. It is due to the prolate deformation driving [431]1/2 Nilsson orbital, intruding from above  $Z = 50$  for large deformation. This phenomenon has been studied and discussed extensively for rhodium isotopes up to  $A = 109$  [10,11]. Experimental evidence for a deformed band in  $^{111}\text{Rh}$  was first proposed by Rogowski *et al.* [12] and later was confirmed on the basis of level lifetime measurements [7]. Since  $^{113}\text{Rh}_{68}$  is near the neutron midshell, this intruder band is expected to be located at low excitation energy and it should be possible to identify some of its members. It is of interest to establish the systematical trend of excitation energy of this band since the minimum seems to be shifted with respect to the neutron midshell [7].

## 1 Experimental procedure

The experiment was carried out at the Ion-Guide Isotope Separator On-Line Facility of the Jyväskylä Accelerator Laboratory (Finland) [5,6,13]. A target of natural  $^{238}\text{U}$ , tilted in order to increase its effective thickness close to  $90\text{ mg/cm}^2$ , was bombarded with 25 MeV protons from the K-130 cyclotron. The intensities were typically of  $10\text{ }\mu\text{A}$ . The neutron-rich fission products of mass  $A = 113$  were on-line mass separated and implanted onto a movable plastic tape viewed by detectors for  $\beta$  and  $\gamma$  radiation. The collection was performed in a cyclic mode chosen to optimize the number of recorded  $^{113}\text{Ru}$  decays ( $T_{1/2} = 0.8\text{ s}$ ), while keeping at a low level the unwanted contributions from longer-lived other  $A = 113$  isobars and of some  $A-16$  impurities formed as molecular beams with  $^{16}\text{O}$ , mainly  $^{97}\text{Y}$ , and their daughters. The beam of  $A = 113$  isobars was collected on the tape for a 1.2 s period and next was blocked for another 1.2 s period. Then the tape was moved and collection was resumed on a refreshed spot of the tape. This 2.4 s data collection cycle is still fairly efficient for the observation of  $^{113}\text{Rh}$  decay ( $T_{1/2} = 2.8\text{ s}$ ).

The low-energy  $\gamma$  spectrum (in the range of 14 to 610 keV) was measured with a LEGe-detector of 1 mm thickness and  $1\text{ cm}^2$  area and the higher range (40 to 2500 keV) with a 37% Ge-detector operated in anticoincidence with a BGO shield. Two 2 mm thick lead plates with a 30 mm hole shielded the BGO shield against direct exposure to the activity. Gating of the Ge-detectors by  $\beta$ -particles was necessary to reject events coming from the laboratory background. Two thin (0.9 mm) plastic scintillators were placed in front of the Ge-detectors to provide the gating signal. In order to avoid false triggers by  $\beta$ -particles and their summing with  $\gamma$ -rays, a coincidence was required between the signals from each Ge-detector and of the plastic  $\beta$  counter on the opposite side of the source. As the detectors were used in a very close geometry to maximize the efficiency, angular correlations effects did not need to be taken into account during data analysis. However, care had to be taken in evaluating coincidence summing and scattering of  $\gamma$ -rays from one detector to the other causing spurious peaks to appear in gated spectra.

Energy and time signals were recorded with the multiparameter system VENLA [14]. Valid events were triggered by any of the  $(\beta\gamma)$ ,  $(\beta X)$ ,  $(\gamma X)$  pairs of events or by the single not  $\beta$ -gated X energy. The latter was required to detect the occasional electromagnetic decay of isomers. A further event parameter was a TDC signal giving the time elapsed since the beginning of the acquisition cycle. Thus, by constructing TDC-energy matrices it was possible to determinate decay half-lives for selected  $\gamma$ -lines using their growth and decay curves. In addition, true singles spectra of the Ge- and LEGe-detectors were recorded by a PC-based independent acquisition system with a threshold of 4 keV in case of the LEGe-detector to extend the range of the detection below the threshold set by the coincidence set-up. The resolution of our  $\beta$ - $\gamma$  timing spectra measured with a TAC was about 6 ns for  $\gamma$  transitions around 200 keV.

### 1.1 Data evaluation

In the range from 200 keV to 600 keV where both Ge-detectors have reasonable efficiency, the adopted intensity values are averages from both Ge ( $\gamma$ ) and LEGe (X) spectra. The average ratio of peak areas corrected by the relative efficiency for transitions in this range yielded the normalization factor needed to extend the calculation of intensities to both the lower- and higher-energy regions where data from a single detector only were of sufficient quality.

Intensities of all transitions up to 600 keV have been corrected for internal conversion using either the available experimental values [4] or using theoretical values [15] under assumption of their most probable multipolarity. In calculation of  $\log ft$  values,  $Q_\beta$  decay energies from [16] were used.

## 2 Results

The  $^{113}\text{Rh}$  level scheme was known up to excitation energies of 1 MeV [4]. We have introduced 61 lines and 20 levels on basis of X- $\gamma$  and  $\gamma$ - $\gamma$  coincidences. Transitions and their coincidence relationships are presented in table 1.

The analysis of  $\beta$ -decay half-lives indicates that there are two groups of  $\gamma$ -lines connected with the 263 and 211 keV lines, with half-lives of 0.9 s and 0.6 s, respectively, see table 2. In ref. [4] these differences were not taken as significant enough to indicate the presence of an isomer in  $^{113}\text{Ru}$  because of the large statistical errors in this first measurement. We assume that the value of 0.6 s results from a small admixture of the 0.9 s half-life ( $^{113}\text{Ru}$  g.s.) in the 0.51 s half-life of  $^{113}\text{Ru}^m$  [2].

The  $^{113}\text{Ru}$  g.s. and isomer half-lives are too close to allow a decomposition of the decay contributions except for the few very intense transitions. We have constructed separate decay schemes of  $^{113}\text{Ru}$  based on the large difference of spins of the ground state ( $I^\pi=5/2^+$ ) [4] and of the isomer ( $I^\pi=11/2^-$ ) [2]. The ground state of  $^{113}\text{Rh}$  is

**Table 1.** Energies, relative intensities and coincidence relations for  $\gamma$ -rays observed in the decay of  $^{113}\text{Ru}$ . Intensities are given as observed for the mixture of ground state and isomer decays. Transitions from levels assumed to be populated by allowed or first-forbidden transitions are labelled by a  $g$  or  $m$  depending on g.s. ( $5/2^+$ ) or isomer ( $11/2^-$ ) decay, respectively. The coincidence list includes lines which are visible in selected gates but are covered in the global projections thus preventing further gating and identification. Tentative levels based on energy sum fitting and partial coincidence relationships are commented but not included in the decay schemes.

$E_\gamma$ (keV)	$I_\gamma^{\text{rel}}$ (%)		Placed		Coincident $\gamma$ -lines
			from	to	
48.1 (1.3)	0.2 (0.2)	$g$	834	787	186, 338, 226
88.1 (0.3)	13.1 (1.3)	$g$	351	263	$K_\alpha(\text{Rh})$ , 88, 206, 228, 263, 482, 627, 683, 710, 1112, 1134, 1161, 1180, 1213, 1227, 1279, 1477, 1535, 1583, 1594, 1615, 1770, 1841, 1870, 1936, 2324
181.0 (0.7)	0.8 (0.4)	$g$	968	786	168, 186, 263, 338
185.8 (0.3)	6.8 (0.8)	$g$	786	601	48, 247, 275, 401, 560 <sup>a</sup> , 1534
206.2 (0.4)	2.7 (0.4)	$g$	785	579	88, 212, 228, 263, 351, 367, 401, 1583
211.7 (0.2)	32.8 (0.8)	$m$	211	0	206, 232, 349, 367, 888, 995, 1180, 1195, 1318, 1632, 1661, 1846, 1911, 1923, 1973, 2157
226.0 (0.7)	0.8 (0.4)	$g$	(1061	834)	
227.6 (0.3)	8.2 (0.4)	$g$	578	351	$K_\alpha(\text{Rh})$ , 88, 206, 263, 351, 1583, 1707
232.3 (0.3)	7.4 (0.3)	$m$	444	211	212, 338, 1923, 1973
233.9 (0.4)	2.7 (0.4)	$g$	834	601	176, 226, 263, 338, 353
246.4 (1.1)	0.3 (0.2)	$b$	(2191	1945)	
247.0 (0.8)	0.6 (0.4)	$g$	(1033	787)	(263)
263.2 (0.2)	100.0 (0.5)	$g$	263	0	$K_\alpha(\text{Rh})$ , (48), 88, 181, 186, 206, 226, 228, 234, (247), 275, 338, 367, 403, 423, 482, 539, 560, 571, 627, 658, 705, 715, 746, 798, 1112, 1133, 1213, 1224, 1368, 1448, 1478, 1549, 1583, 1594, 1615, 1646, 1770, 1841, 1858, 1928, 1936, 1958, 2024, 2035, 2324, 2360
274.7 (0.7)	0.9 (0.1)	$g$	1061	787	88, 161, (100), (163), 164 <sup>c</sup> , 186, 190, 263, 338
337.6 (0.3)	23.4 (0.4)	$g$	601	263	(48), (181), 186, (226), 234, 247, 263, 275, 367, 401, 560 <sup>a</sup>
351.2 (0.3)	11.8 (1.7)	$g$	351	0	206, 226, 228, 482, 538, 658, 1770
367.1 (0.5)	2.1 (0.2)	$g$	579	212	206, 212
367.2 (0.5)	2.9 (0.4)	$g$	968	601	263, 338
401.0 (0.7)	1.1 (0.1)	$d$			( $K_\alpha(\text{Rh})$ ), 88, 117, 152, 186, 263
403.4 (0.5)	2.4 (0.5)	$ge$	(2525	2121)	$K_\alpha(\text{Rh})$ , 217, 263
422.9 (0.5)	2.3 (0.1)	$f$			( $K_\alpha(\text{Rh})$ ), 88, 162, 263, (338)
443.9 (0.4)	5.5 (0.2)	$m$	444	0	138, 161, 166, 1923, 1973
482.0 (0.8)	0.7 (0.2)	$g$	834	351	$K_\alpha(\text{Rh})$ , 88, 226, 263, 351
560.1 (0.4)	5.1 (0.2)	$g$	823	263	$K_\alpha(\text{Rh})$ , (85), (88), (217), 263
571.1 (0.4)	6.6 (0.2)	$g$	834	263	263, (352) <sup>h</sup>
578.7 (0.6)	1.9 (0.2)	$g$	(579	0)	(84), (349)
600.5 (0.5)	2.1 (0.3)	$g$	601	0	185
626.8 (0.5)	2.3 (0.1)	$g$	978	351	88, 263
657.8 (0.5)	2.5 (0.1)	$g$	1009	351	88, 263, 351
682.8 (0.8)	0.7 (0.2)	$g$	(1033	351)	(88)
704.9 (0.7)	0.9 (0.1)	$g$	968	263	263
709.4 (0.5)	2.7 (0.1)	$g$	(1061	351)	88
715.1 (0.4)	5.8 (0.1)	$g$	978	263	263
745.9 (0.5)	2.4 (0.1)	$g$	1009	263	263
770.9 (0.7)	1.2 (0.1)	$g$	1033	263	263
785.0 (0.5)	2.7 (0.2)	$g$	(785	0)	(161)
797.8 (0.6)	2.3 (0.1)	$g$	1061	263	263
888.1 (0.8)	0.9 (0.4)	$m$	(2417	1530)	
906.2 (0.8)	0.8 (0.1)	$g$	(1485	579)	88
994.7 (0.5)	3.3 (0.4)	$m$	1205	212	(212), (333)
1008.7 (0.6)	2.9 (0.2)	$g$	(1009	0)	263 <sup>h</sup>
1061.2 (0.6)	2.5 (0.2)	$g$	(1061	0)	(263) <sup>h</sup>
1112.2 (1.0)	0.5 (0.4)	$g$	1463	351	88, (212) <sup>h</sup> , 263
1123.0 (0.8)	0.9 (0.1)	$g$	(1909	785)	(212)
1133.9 (0.8)	1.1 (0.3)	$gi$	1485	351	(88), (190), 263
1160.8 (0.9)	0.7 (0.1)	$g$	(2222	1061)	(88), (212)

Table 1. Continued.

$E_\gamma$ (keV)	$I_\gamma^{\text{rel}}$ (%)		Placed		Coincident $\gamma$ -lines
			from	to	
1180.4 (0.7)	1.4 (0.7)	<i>g</i>	(1966	785)	88, 190, 212, 263
1194.6 (0.6)	2.6 (0.2)				135, 212, 263
1213.1 (0.7)	1.3 (0.1)	<i>g</i>	(2222	1009)	88, 263
1223.3 (0.7)	1.7 (0.2)	<i>g</i>	(2191	968)	
1225.0 (1.0)	0.6 (0.4)	<i>m</i>	(2057	834)	
1226.6 (0.6)	3.7 (0.1)	<i>ge</i>	(2287	1061)	88, 190
1318.4 (0.7)	1.4 (0.1)	<i>m</i>	1530	212	212
1367.6 (0.6)	2.9 (0.1)	<i>gj</i>	2191	823	(212), 263 <sup>h</sup> , (560)
1448.4 (0.9)	0.8 (0.8)	<i>gln</i>	(1711	263)	(263)
1464.3 (1.0)	0.7 (0.1)	<i>g</i>	(1463	0)	
1534.6 (1.1)	0.5 (0.1)	<i>m</i>	(2368	834)	88, (263)
1548.9 (0.7)	1.7 (0.1)	<i>ge</i>	(2525	978)	(88), (206), (263)
1583.1 (0.6)	3.6 (0.2)	<i>m</i>	2368	784	88, 206, 263
1593.8 (0.7)	2.4 (0.2)	<i>g</i>	1945	351	88, 263
1614.7 (0.8)	1.4 (0.1)	<i>g</i>	1966	351	88, 263
1631.7 (0.6)	4.8 (0.3)	<i>m</i>	1843	212	212
1645.7 (0.7)	2.7 (0.2)	<i>g</i>	1909	263	263
1661.2 (1.0)	0.6 (0.1)				88, 212
1770.2 (0.7)	2.7 (0.3)	<i>g</i>	2122	351	88, 263, (351)
1840.8 (0.7)	2.9 (0.2)	<i>g</i>	2191	351	88, (212) <sup>h</sup> , 263, (351)
1846.1 (0.8)	1.8 (0.1)	<i>m</i>	2057	212	212
1858.1 (0.7)	3.4 (0.2)	<i>g</i>	2122	263	263
1869.7 (0.7)	2.3 (0.2)	<i>g</i>	2222	351	( $K_\alpha(\text{Rh})$ ), 88
1911.0 (0.9)	1.1 (0.1)	<i>g</i>	2122	212	212
1922.9 (0.7)	3.6 (0.1)	<i>m</i>	2368	444	212, 232
1927.6 (0.7)	4.5 (0.2)	<i>g</i>	2191	263	263
1936.3 (1.0)	0.7 (0.3)	<i>ge</i>	(2287	351)	(88)
1957.8 (0.7)	3.6 (0.3)	<i>g</i>	2222	263	263
1973.2 (0.6)	8.3 (0.2)	<i>m</i>	2417	444	212, 232, 444
2023.9 (1.0)	0.9 (0.4)	<i>ge</i>	(2287	263)	
2034.5 (1.0)	0.8 (0.1)	<i>g</i>	2298	263	(263)
2058.4 (1.3)	0.3 (0.3)	<i>m</i>	(2057	0)	
2121.8 (1.1)	0.7 (0.1)	<i>g</i>	(2122	0)	
2156.5 (1.1)	0.7 (0.1)	<i>m</i>	2368	212	(212)
2173.6 (1.2)	0.5 (0.1)	<i>ge</i>	(2525	351)	
2191.0 (0.8)	2.9 (0.1)	<i>g</i>	2191	0	
2297.1 (0.9)	1.7 (0.3)	<i>g</i>	2298	0	
2324.0 (1.3)	0.3 (0.1)	<i>gn</i>	(2675	351)	(88)
2360.4 (0.9)	1.8 (0.2)	<i>gn</i>	(2623	263)	(263)
2368.0 (0.9)	1.6 (0.1)	<i>m</i>	2368	0	
2417.6 (1.0)	1.1 (0.1)	<i>m</i>	2417	0	

<sup>a</sup> Coincidences could indicate another 560 keV line.

<sup>b</sup> Transition energy fits between levels 2368–2121.

<sup>c</sup> Transition in decay of <sup>113</sup>Tc.

<sup>d</sup> Transition energy fits between levels 2368–1966.

<sup>e</sup> Tentative level (not shown on the scheme) based on energy fitting of 3 transitions.

<sup>f</sup> Transition energy fits between levels 2368–1945.

<sup>h</sup> Coincidence against proposed placement.

<sup>i</sup> Transition energy fits between levels 1966–834.

<sup>j</sup> Transition energy fits between levels 1945–579.

<sup>l</sup> Transition energy fits between levels 2417–968.

<sup>n</sup> Tentative level based on a single weak coincidence.

**Table 2.** Half-lives observed for transitions in  $^{113}\text{Ru}$  decay. The values result from the superposition of g.s. and isomer decays. Based on the spins of the levels they de-excite, the half-lives for the transitions of 212 and 232 keV are representative of the half-life of the high-spin  $^{113}\text{Ru}^m$  and the 263 keV transition of the low-spin ground state.

Energy (keV)	$T_{1/2}$ (s)	Detector
$K_\alpha(\text{Rh})$	$0.66 \pm 0.32$	LEGe
88.1	$0.94 \pm 0.30$	large Ge
	$0.82 \pm 0.06$	LEGe
211.7	$0.61 \pm 0.16$	large Ge
	$0.64 \pm 0.03$	LEGe
232.3	$0.61 \pm 0.11$	LEGe
263.2	$0.88 \pm 0.30$	large Ge
	$0.93 \pm 0.05$	LEGe

assumed  $I^\pi = 7/2^+$  from systematics. The conversion coefficients  $\alpha_K(211) = 0.06(2)$  and  $\alpha_K(263) = 0.033(5)$  reported in ref. [4] are consistent with  $M1(+E2)$  and pure  $E2$  multiplicities, respectively, which are strongly suggested by the presence of a  $9/2^+$  and of a  $3/2^+$  state in this energy region in all lighter odd-mass rhodium isotopes. Consequently, we assume that levels with a decay to the  $3/2^+$  level at 263.1 keV have  $I \leq 7/2$  and must be directly populated in the decay of the low-spin  $^{113}\text{Rh}$  ground state only. On the other hand, levels with a branch to the  $9/2^+$  level at 211.6 keV and without transitions to the  $3/2^+$  at 263.1 keV nor to the proposed 351.2 keV  $5/2^+$  level are assumed to be populated in the high-spin decay only. This procedure obviously must be arbitrary at some point, as for instance, feeding of  $7/2$  states and possibly of  $5/2$  states could occur from the high-spin isomer via high-energy cascades which might have escaped detection. A small fraction of the observed  $\gamma$ -ray intensity, about 18 relative units of the 365 in total, has not been placed in the schemes. The separate decay schemes are shown in figs. 1 and 2.

The centroid shifts obtained from  $\beta$ - $\gamma$ - $t$ -delayed coincidences are shown in fig. 3 for selected transitions. The prompt curve was obtained by combining the centroid positions of high-lying lines in both  $^{113}\text{Rh}$  and  $^{113}\text{Pd}$  level schemes, thus assumed not to display measurable centroid shifts, with lines of  $A = 111$  activities measured in a separate control run using for reference half-lives given in [7], and some lines due to the  $A = 97$  activities present in the beam as oxides. The uncertainty in the 200–400 keV range is estimated to be near 0.15 ns.

Definite shifts are observed for the lines at 211.7, 263.1 and 337.6 keV. They convert into half-lives of 0.21(13) ns, 0.51(11) ns and 0.66(14) ns, respectively. However, for the 263.1 keV transition the experimental half-life is a superposition of the own lifetime of the 263.1 keV level and of the lifetime of the 600.7 keV level decaying to the 263.1 keV level via the 337.6 keV transition. Using  $\gamma$ -ray intensities as listed in table 1 one deduces  $\tau_{263}(\text{exp}) = \tau_{263} + 0.19\tau_{600}$ , yielding  $t_{1/2}(263) = 0.38(12)$  ns.

## 2.1 Levels fed in $^{113}\text{Ru}$ ground-state decay

There is some uncertainty about the magnitude of the  $\beta$  feeding to the ground state which as a  $5/2^+$  to  $7/2^+$  transition is allowed. In ref. [4] a negligible branching was adopted, in fact depending on the assumption of a weak ground-state branch for the daughter decay of  $^{113}\text{Rh}$  to  $^{113}\text{Pd}$ . However, this branch is also of allowed character ( $7/2^+ \rightarrow 5/2^+$ ) and considerations about relative yields obtained for  $A = 113$  isobars rather suggested a sizeable value [3]. A very weak g.s. branching in  $^{113}\text{Ru}$  decay is indeed at variance with the systematics of these transitions. The  $\log ft$  values for the less neutron-rich ruthenium g.s. decays are of about 6 [17] and are even lower for  $^{111}\text{Ru}$  decay, for which  $\log ft = 5.0$  is adopted in ref. [7]. Nevertheless, since these yield considerations are based on smooth distributions *versus*  $Z$  and therefore are not purely experimental, we have calculated the  $\beta$  branchings neglecting the g.s. branch according to ref. [4]. Thus, a probable increase of  $\log ft$  values (of the order of 0.3) for the excited states has to be kept in mind especially when dealing with parity assignments based on the allowed or first-forbidden character of the transitions.

The 263.1 keV level is established as a  $3/2^+$  level, as mentioned above. The half-life of 0.38(12) ns is in good agreement with a preliminary value of 0.49(19) ns [7]. The  $E2$  transition is thus enhanced with respect to the single-particle estimate by a factor of 33(8).

The 351.2 keV level has a very strong link to the 263.1 keV level and a weaker one to the  $7/2^+$  ground state. The analogy with the 382.1 keV level in  $^{111}\text{Rh}$  suggests  $I^\pi = 5/2^+$ . In both nuclei, the allowed  $5/2^+$  to  $5/2^+$   $\beta$  transition is substantially hindered. There is some feeding from the high-spin isomer via  $\gamma$ -rays.

The 578.8 keV level decays to  $5/2^+$ ,  $7/2^+$  and  $9/2^+$  levels. The strongest branch is to the 351 keV level, suggesting  $I^\pi = 7/2^+$  by analogy with the 632.4 keV level in  $^{111}\text{Rh}$ . There is also some feeding from the high-spin isomer via  $\gamma$ -rays.

The 600.7 keV level has a very strong branch to the  $3/2^+$  level at 263.1 keV. It is similar to the  $I^\pi = 3/2^+$  level at 395.0 keV in  $^{111}\text{Pd}$ . The level half-life of 0.66(14) ns shows that the  $E2$  transition to the ground state (with a branching ratio of 0.082) is retarded by a factor of about 36 with respect to the s.p. unit.

The 784.9 keV level is only weakly fed by  $\gamma$ -rays from levels possibly populated in both  $^{113}\text{Ru}$  decays. It has branches only to  $7/2^+$  levels, which makes an assignment to one or the other decay possible. We have assumed that it belongs to the low-spin decay.

The 786.5 keV level is found to decay only to the 600.7 keV level suggested as a  $3/2^+$  state. Feeding transitions seem to belong to the low-spin decay, in agreement with the upper spin limit of  $7/2$ .

The 823.3 keV level decays only to the lowest  $3/2^+$  state, which also puts an upper limit of  $7/2$  and assigns it to this decay.

The 834.4 keV level decays to low-spin ( $I \leq 5/2$ ) levels. It is nevertheless populated by  $\gamma$  transitions belonging to the low- and the high-spin decays.

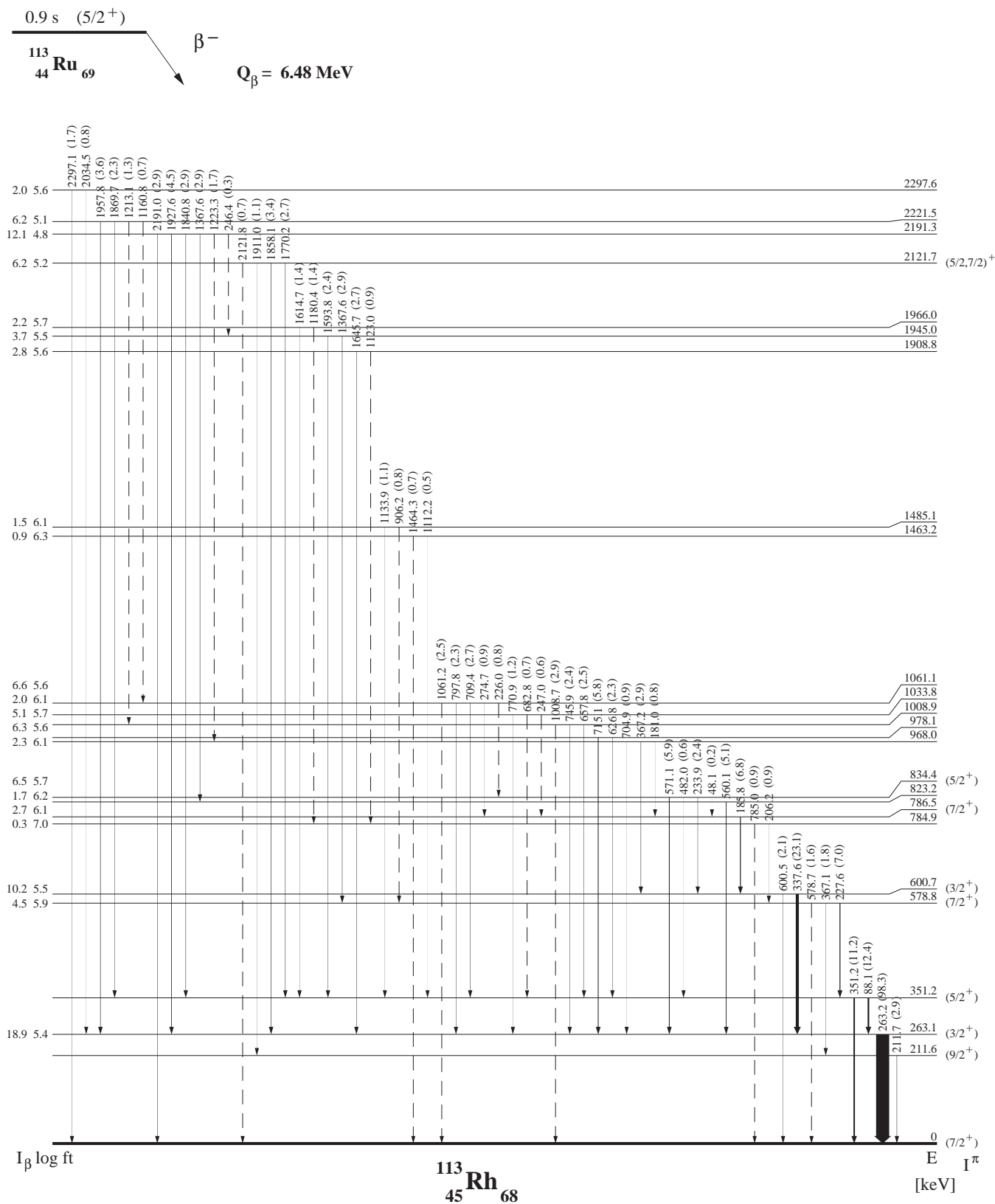


**Fig. 1.** The decay scheme of the <sup>113</sup>Ru ground state. Unique spin and parity assignments are based on systematics. See text for details.

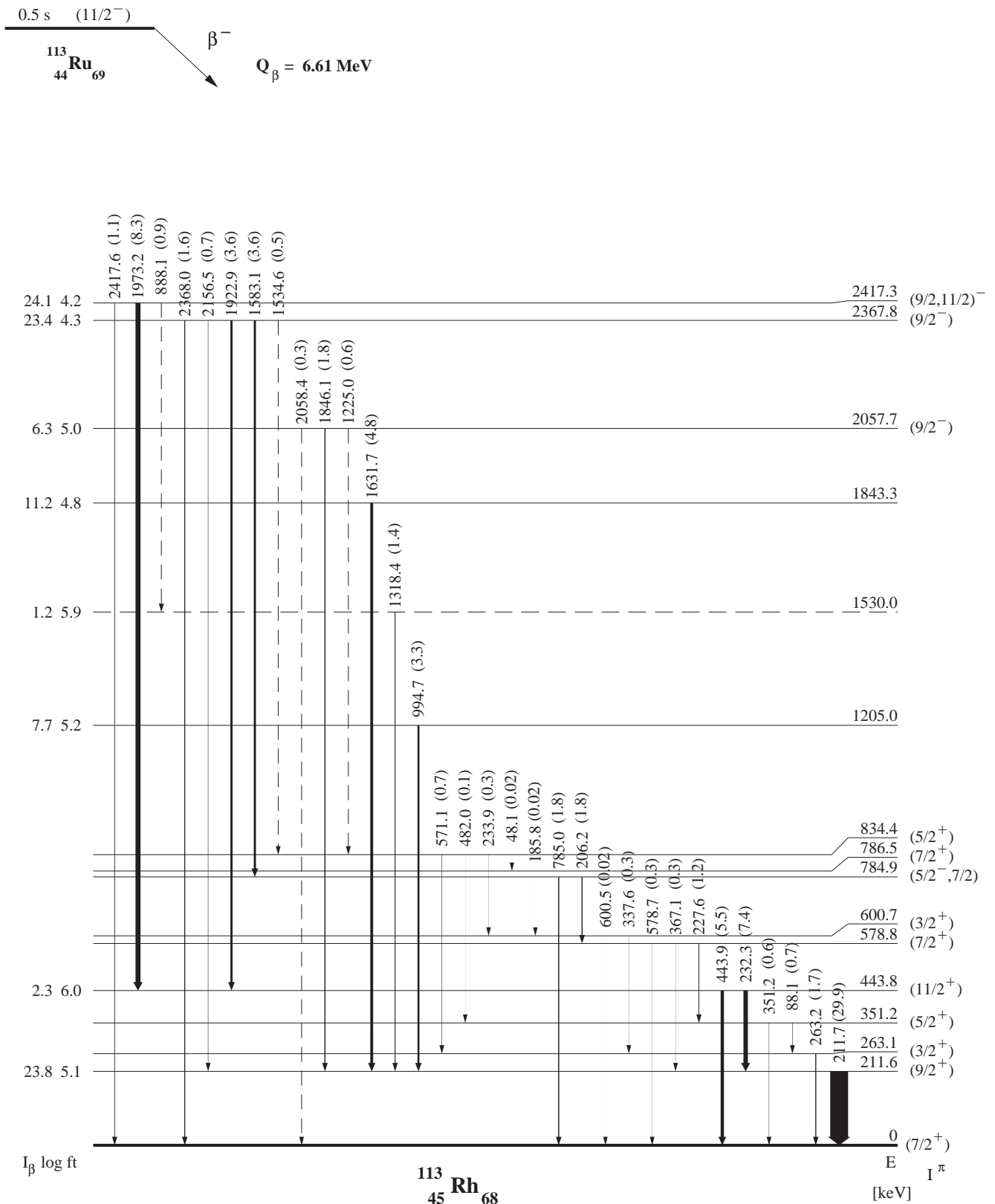


**Fig. 2.** The decay scheme of the <sup>113</sup>Ru isomer. Unique spin and parity assignments are based on systematics. See text for details.

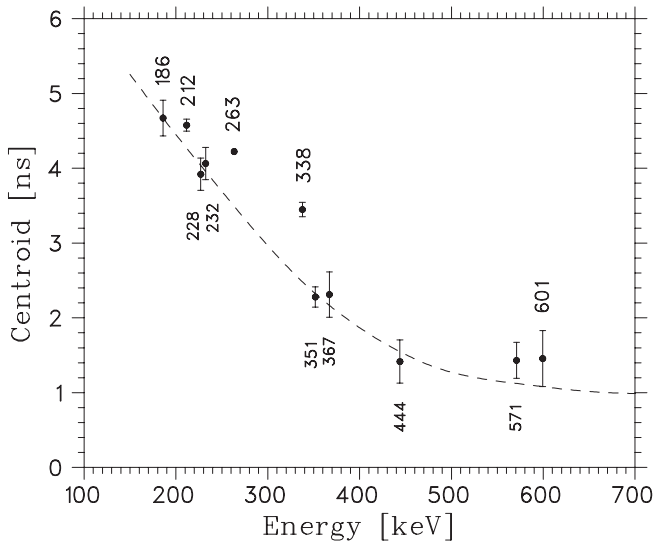


**Fig. 3.** Centroid plot for the  $\beta$ - $\gamma$ -time spectra versus transition energy in the Ge-detector for the most intense transitions in  $^{113}\text{Rh}$ . The dashed curve represents the location of centroid positions for transitions with negligible half-lives, the so-called prompt curve. See text for details.

Other levels have a transition to the 263.1 keV level. Thus, the levels at 968.0, 978.1, 1008.9, 1033.8, 1061.1, 1908.8, 2121.7, 2191.3, 2221.5 and 2297.6 keV belong to the low-spin decay. In addition, the levels at 1463.2, 1485.1, 1945.0 and 1966.0 keV are included in this decay scheme since they have a transition to the 351.2 keV level assumed as  $5/2^+$  but no transition to the  $9/2^+$  211.6 keV level has been observed. This makes a spin larger than  $7/2$  rather unlikely. Finally, some tentative levels could belong to this decay also. They are levels at 1711.5, 2287.7, 2324.2, 2360.5 and 2525.0 keV (not shown on the scheme).

## 2.2 Levels fed in $^{113}\text{Ru}$ high-spin isomer decay

In this decay, ground-state  $\beta$  feeding is not likely to be very high due to the large spin difference and change of parity. It is accordingly neglected. The 211.6 and 443.8 keV levels have been seen in  $^{248}\text{Cm}$  prompt fission [18] creating a band structure.

The 211.6 keV level has spin  $9/2^+$ , this assignment being made first by Penttilä *et al.* [4] on the basis of the  $M1 + E2$  multipolarity of the g.s. transition. The  $\log ft$  value of 5.1 is, however, much too low for the  $11/2^- \rightarrow 9/2^+$  first-forbidden transition. It could be that still a large fraction of the  $\gamma$ -ray feeding to the 211.6 keV level has been overlooked due to its high energy and fragmentation into many branches. This general phenomenon [19] is expected to play a part especially in the high-spin ruthenium decay. There, most low-lying levels cannot be strongly populated due to the spin difference. Thus, a large fraction of the  $\beta$ -decay intensity must go to high-energy levels. Nevertheless, the  $\beta$ -feeding is cancelled if adding a bit less than 10 relative intensity units while 18 units have not been placed in the schemes. For these reasons, it does

not seem necessary yet to revise the  $11/2^-$  assignment for  $^{113}\text{Ru}$  [2].

The 443.8 keV level is assumed to be the  $11/2^+$  state [18]. Such a level has not been reported in the lighter rhodium isotopes. This can be explained by the absence of a high-spin  $\beta$ -decaying ruthenium parent.

Levels with a branch to the  $9/2^+$  level at 211.6 keV and without transitions to the  $3/2^+$  at 263.1 keV and the proposed 351.2 keV  $5/2^+$  level are assumed to be populated in the high-spin decay only. These are the levels at 1205.0, 1530.0, 1843.3, 2057.7, 2367.8 and 2417.3 keV. The 2367.8 and 2417.3 keV levels have transitions to the  $7/2^+$  ground state, which can be explained if they have  $I^\pi = 9/2^-$ . The 2367.8 keV level also has links to the 784.9 and 834.4 keV levels fed in  $^{113}\text{Ru}$  g.s. decay. The 784.9 keV level thus has  $I^\pi = (5/2^-, 7/2)$ . The 834.4 keV level which has a transition to the  $3/2^+$  state could have  $I = (5/2, 7/2)$ , since the  $M2$  multipolarity cannot be excluded for the weak 1534.6 keV feeding transition.

## 3 Discussion

A number of interesting phenomena are observed for the neutron-rich nuclei around mass  $A = 100$ – $110$ . These are shape coexistence [20], triaxiality [21], and existence of low-lying intruder states [7, 22]. Predicted values of axially symmetric quadrupole deformation parameter  $\beta_2$  [23] for  $36 < Z < 48$ ,  $61 < N < 73$  show a prolate to oblate shape transition in the vicinity of  $N = 66$  whereas another calculation [24] predicts the same shape transition at about  $N = 60$ . For nuclei in the current region of interest potential energy minima for prolate and oblate shapes are separated by a low barrier and there is a trend to favour triaxially deformed shapes. Relative depths and equilibrium deformation of potential minima for prolate and oblate shapes may be different. Nevertheless, experimental energies of first  $2^+$  excited states from strontium to cadmium behave in a rather smooth way if one excepts the region of shell closures near  $^{96}\text{Zr}$  extending up to  $N \simeq 60$ .

Systematics of  $11/2^-$  states in odd-neutron nuclei from ruthenium to tin for  $61 < N < 73$  shows smooth tendency of lowering and then increasing their energy keeping isomeric character, except for ruthenium [4, 17, 25]. Thus, the 0.5 s state at  $130 \pm 30$  keV in  $^{113}\text{Ru}$  could be a  $11/2^-$  isomeric state [2], although breaking the increasing energy trend of energies in ruthenium isotopes.

The level structure of neutron-rich odd-mass rhodium isotopes has been discussed extensively for  $A \leq 109$  based on detailed experiments [10, 11] and recently for  $A = 111$ , the scheme of which was investigated by some of us [7]. For the very neutron-rich isotope  $^{113}\text{Rh}$ , the only information available is from decay data in ref. [4] and this work. The discussion will be limited to the identification of levels as assigned in this work, on basis of arguments of excitation energies and branching ratios systematics.

### 3.1 Spherical levels in $^{113}\text{Rh}$

The ground state ( $7/2^+$ ), the 211 keV ( $9/2^+$ ), 263 keV ( $3/2^+$ ), 351 keV ( $5/2^+$ ) and 579 keV ( $7/2^+$ ) levels fit very



well in the systematics of energies and branching ratios that, in turn, was used to assign spin and parity of the last two ones. Their structure obviously involves the  $g_{9/2}$  proton, itself identified with the first excited state.

By analogy with Ag isotopes exhibiting a low-lying  $7/2^+$  state, the Rh ground states should involve the seniority  $v = 3$  state based on  $g_{9/2}$  protons. According to V. Paar [9] the  $v = 1$  to  $v = 3$  transition is characterized by a large  $E2/M1$  ratio due to retardation of the  $M1$  and enhancement of the  $E2$  components. The measured conversion coefficient of 0.06(2) for the 211.6 keV transition [4] ( $\alpha_K(M1) = 0.040$ ,  $\alpha_K(E2) = 0.078$ ) indeed allows a large  $E2$  admixture. It is, however, too inaccurate to extract a meaningful  $\delta^2$  value. We note that  $\alpha_K = 0.06$  corresponds to  $\delta^2 = 1$ . Using this value and the half-life of 0.21(13) ns one obtains  $B(M1) = 0.006$  and  $B(E2) = 100$  W.u., which gives the expected —maybe with somewhat extreme values in this case— orders of magnitude according to the systematics of these transitions. For the corresponding transition in  $^{111}\text{Rh}$ , of 211.4 keV,  $\alpha_K = 0.037(3)$  [4] and  $t_{1/2} < 0.5$  ns [7] are reported. These properties are indeed similar. For a detailed discussion, it will be however necessary to improve significantly the measurements of mixing ratios and lifetimes for the whole chain of odd- $A$  rhodium isotopes. Here, it is to mention that although the spherical interpretation is in accordance with data for Rh isotopes close to stability [10, 11], a deformed interpretation of the  $7/2^+$  and  $9/2^+$  levels in the most neutron-rich rhodium isotopes has recently been put forward by the EUROGAM Collaboration. This interpretation is based on the observation of band structure using fission induced by heavy ions [26].

The other states of even parity must involve couplings of the  $v = 1$  and  $v = 3$  states with core excitations. The 263.1 keV  $E2$  transition from the  $3/2^+$  level is enhanced by 33(8) times. This compares with the lower limit of 7 for the corresponding level at 303.6 keV in  $^{111}\text{Rh}$  [7]. This enhancement is similar to those in the neighbouring cores of  $^{112}\text{Pd}$  and  $^{114}\text{Pd}$ , in which the  $2^+ \rightarrow 0^+$  transitions are accelerated by factors of 39(7) and 21(7), respectively [17]. This supports the interpretation of the  $3/2^+$  level as due to coupling of the  $7/2^+$  ground state with the  $2^+$  state of the even-even core.

The 444 keV  $I^\pi = 11/2^+$  level is a probable other member of a similar core + particle coupling multiplet. Here both  $7/2^+$  and the  $g_{9/2}$  single proton can contribute to the wave function. The systematics also predicts a number of odd-parity levels based on the  $p_{1/2}$  proton and its couplings with core excitations, forming a  $(3/2^-, 5/2^-)$  doublet near the  $2^+$  core energy about 300 keV above the single  $p_{1/2}$  state. As shown in ref. [7] the  $p_{1/2}$  level and its couplings to phonon states move upwards with increasing neutron number. In contrast, another  $(3/2^-, 5/2^-)$  doublet of states keeps its energy rather constant near 800 keV above the ground states. These states are the  $p_{3/2}$  and  $f_{5/2}$  proton holes identified by transfer reaction in the lighter mass rhodiums up to  $A = 109$  [10, 11]. The energy systematics suggests that a first crossing of  $(3/2^-, 5/2^-)$  doublets occurs in  $^{109}\text{Rh}$ . The upwards going  $2_2^+ \otimes p_{1/2}$

states of the second  $2^+$  core phonon are possibly the 860 and 977 keV levels in  $^{111}\text{Rh}$  while the presumably lower-lying proton-hole states have not been identified. A second crossing is expected to occur in  $^{113}\text{Rh}$  where the  $2_1^+ \otimes p_{1/2}$  states built on the first phonon should reach the energies assumed for the  $p_{3/2}$  and  $f_{5/2}$  hole states. Thus, the extrapolation for mass  $A = 113$  predicts the  $p_{1/2}$  state near 600 keV, while two  $(3/2^-, 5/2^-)$  doublets are expected near 800 keV. There is neither level candidate for the  $p_{1/2}$  proton state nor for a  $3/2^-$  level near 800 keV. There is a potential candidate for a  $5/2^-$  state only as the 784.9 keV level. The failure to find such states might be partially due to the low statistics for this exotic decay but also to their higher excitation energy which prevents strong population via  $\gamma$ -rays from the high-lying even-parity levels.

### 3.2 Deformed levels in $^{113}\text{Rh}$

The systematic occurrence of a  $K = 1/2$  band of even parity in the odd-mass rhodium, silver and indium isotopes is well known [10, 11, 27, 28]. The [431]1/2 Nilsson orbital has a large slope that drives deformation to be prolate for particle-hole configurations in nuclei with  $Z < 50$ . In the neutron-rich rhodium isotopes with  $A > 107$  the  $K = 1/2$  band has a large and negative decoupling parameter so that there is an inversion of spins, the lowest state being the  $I = K + 1 = 3/2$  band member. An interesting feature of this band is that the minimum of excitation energy occurs in  $^{109}\text{Rh}$  rather than in  $^{111}\text{Rh}$  at the  $N = 66$  neutron midshell. In that respect it deviates from the  $K = 1/2$  band in silver isotopes and other intruder bands for  $Z \geq 47$ . However, this shift has been observed recently for intruder bands in even-even palladium isotopes [22]. Level energies and deformations extracted from  $B(E2)$  values in even-even Sr, Zr, Mo and Ru isotopes [17] indeed suggest a maximum to occur at lower neutron number. For instance we note the saturation of deformation at  $\beta = 0.4$  after  $N = 60$  in strontium isotopes [29] and, closer to rhodium, the deformations measured for  $^{108}\text{Ru}$  ( $\beta = 0.27$ ) and  $^{110}\text{Ru}$  ( $\beta = 0.29$ ) [30]. Thus, when  $Z$  is decreasing below 46, there appears a shift of the location of the maximum deformation to lower  $N$  (going farther from the midshell) and an increase of its magnitude.

The 601 keV level exhibits branching ratios strongly suggesting the  $3/2^+$  band head. Moreover, the  $E2$  ground-state transition is retarded by a factor of 36(8) comparing with 83(8) for the corresponding level at 395 keV in  $^{111}\text{Rh}$  [12]. A smaller hindrance indeed seems reasonable since with higher excitation energy the configuration might become more mixed. The level energy is fitting well into a simple extrapolation of energy systematics.

The 786.5 and 834.4 keV levels are in the energy range expected for the next  $7/2^+$  and  $5/2^+$  states. The 834.4 keV level has a strong branch to the 600.7 keV  $3/2^+$  level and is linked to the 786.5 keV level via the 48.1 keV transition. Moreover, the only observed decay of the 786.5 keV level is to the 600.7 keV level. This gives a hint for the existence of a band based on the 600.7 keV level and including the

**Table 3.** Energy parameters for the  $K = 1/2$  bands in nuclei  $^{111}\text{Rh}$  and  $^{113}\text{Rh}$ . Free parameters are a constant energy, the leading term  $a_I$  in  $I(I+1) - K^2$  and the staggering term  $A_{2K}$ . The  $K = 1/2$  band head in  $^{113}\text{Rh}$  is predicted at 621 keV.

$I$	$^{111}\text{Rh}$		$^{113}\text{Rh}$	
	Energy (keV)		Energy (keV)	
	Exper.	Fit	Exper.	Fit
1/2	440.5	440.5		(620.7)
3/2	395.0	398.3	600.7	600.3
5/2	663.1	664.5	834.4	834.5
7/2	567.5	566.1	786.5	786.9
$a_I$	19.6		20.0	
$A_{2K}$	-33.65		-26.83	

786.5 keV ( $7/2^+$ ) and 834.4 keV ( $5/2^+$ ) levels. In this interpretation the 185.8 keV transition must be a collective  $E2$  transition as  $7/2^+ \rightarrow 3/2^+$ . The lifetime expected assuming one s.p. unit for the transition probability is 77 ns. Since enhancements as high as 200 have been reported for such intraband  $E2$  transitions in  $^{109}\text{Rh}$  and  $^{111}\text{Rh}$  [7,11] the actual half-life could be of the order of 0.3 ns. This is the sensitivity of the experimental method and, indeed, there is no definite centroid shift for the 185.8 keV line in fig. 3. Thus, the lack of a measurable half-life, while no definite proof for the interpretation, is consistent with regarding 185.8 keV as an intraband  $E2$  transition.

Table 3 compares the energies and parameters of the band in  $^{111}\text{Rh}$  and of the band in  $^{113}\text{Rh}$  as proposed from the above considerations. The fit of the 3 selected  $^{113}\text{Rh}$  levels yields values for the leading term in the moment of inertia  $a_I$  and the staggering term  $A_{2K}$  close to those for the band in  $^{111}\text{Rh}$ . The leading terms  $a_I$  both imply moments of inertia close to 45% of the rigid rotor value. When rescaled by  $A^{5/3}$  the moment of inertia of  $^{113}\text{Rh}$  is slightly smaller than for  $^{111}\text{Rh}$ . It is logical to observe the largest moment of inertia and lowest excitation energies of the intruder band near midshell, both being related to deformation. A level candidate for the predicted  $1/2^+$  band head is not observed. As a matter of fact, such low-spin levels are too weakly populated as is shown by our failure to identify the  $p_{1/2}$  also expected in this energy range.

### 3.3 Beta-decay of $^{113}\text{Ru}$

In both  $^{113}\text{Ru}$  ground state and isomer decays, feeding to the states below 1.8 MeV is rather weak and the  $\beta$  strength is concentrated around levels with 2.3 MeV excitation energy, see figs. 4 and 5. A similar pattern is observed for the decay of  $^{111}\text{Ru}$  ( $I^\pi = 5/2^+$ ) [7] that corresponds to the low-spin state of  $^{113}\text{Ru}$ . In that case, in spite of a 50% branching to the rhodium ground state, there are some very low  $\log ft$  values for transitions to high-lying levels, e.g., 4.8 (1898 keV), 4.6 (2034 keV) and 5.0 (2127 keV). In  $^{113}\text{Ru}$   $5/2^+$  decay there are also several low  $\log ft$  values,

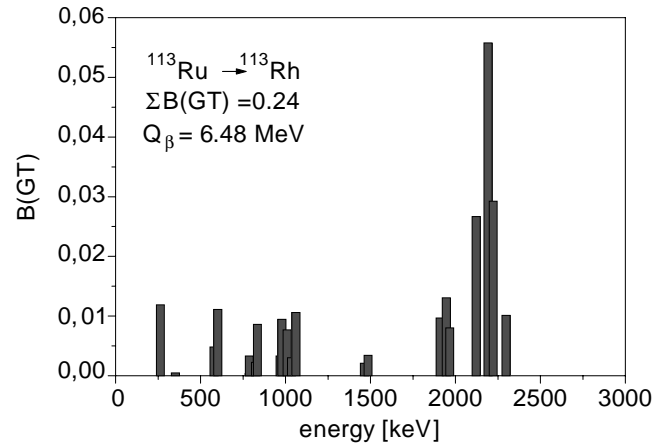


**Fig. 4.**  $B(\text{GT})$  strength distribution for decay of the  $I^\pi = 5/2^+$  ground state of  $^{113}\text{Ru}$  calculated without direct feeding of the  $7/2^+$   $^{113}\text{Rh}$  g.s., see text for details.

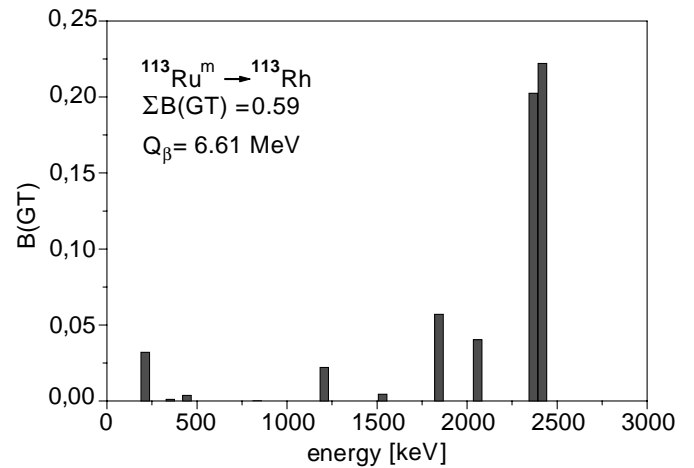


**Fig. 5.**  $B(\text{GT})$  strength distribution for decay of the  $I^\pi = 11/2^-$  isomeric state in  $^{113}\text{Ru}$ .

5.2 (2121 keV), 4.8 (2191 keV) and 5.1 (2222 keV). However, these are calculated with no direct feeding of the ground state. As it was mentioned above, it is probable that there is a sizeable ground-state branch in which case these values might increase. Thus, the decay of  $^{113}\text{Ru}$  to high-lying levels seems to be somewhat slower than  $^{111}\text{Ru}$  decay. The feedings to the lowest levels are perturbed by the superposition of both ground state and isomer decay of  $^{113}\text{Ru}$  and are dependent on the decomposition of the intensities. The adopted values nevertheless are consistent with the spins and parities as they have been proposed. The large feeding ( $\log ft = 5.5$ ) to the 600.7 keV level, the  $3/2^+$  level of the  $K = 1/2$  band is quite unexpected, if compared with the decay of  $^{111}\text{Ru}$ . If, as suggested by the calculated energy for the  $K = 1/2$  band head at 621 keV, there is extra feeding via a converted  $1/2^+ \rightarrow 3/2^+$  transition, this direct feeding will somewhat decrease.

The decay of the  $^{113}\text{Ru}$  high-spin level clearly favours two high-lying states at 2368 keV and 2417 keV, with  $\log ft = 4.3$  and 4.2 respectively, while there are additional levels with still low  $\log ft$  values such as the levels

**Table 4.** Sums of GT strengths for ruthenium isotopes.

<i>A</i>	<i>B</i> (GT)	Ref.
108	0.34	[32]
110	0.26	[32]
111	0.22	[7]
112	0.23	[32]
113	0.24	This work
113 <sup>m</sup>	0.59	This work

at 1843 keV (4.8) and 2058 keV (5.0). This indicates faster transitions than for the  $5/2^+$  decay. There is a large feeding to the  $9/2^+$  level at 211.6 keV although the transition should be first forbidden. The  $\log ft$  value after decomposition of the intensity of the 211.6 keV  $\gamma$  transition is 5.1. We have mentioned that this large feeding could be due to unplaced or unobserved  $\gamma$ -ray intensity. Alternatively, no available experimental data seems to prevent a new assignment of  $9/2^-$  instead of  $11/2^-$  for  $^{113}\text{Ru}$ . It would allow a different decomposition of the  $\beta$ -decay intensity in which  $7/2$  states are fed by decay of both low- and high-spin ruthenium. In that way, a larger fraction of the  $\gamma$ -intensity could populate the  $9/2^+$  state, thereby decreasing the amount of requested direct  $\beta$  feeding and consequently increasing the  $\log ft$  value.

For both decays of  $^{113}\text{Ru}$  nucleus the decay has to involve a  $g_{7/2}$  neutron inside of a  $0^+$  pair, changing to a  $g_{9/2}$  proton. The odd  $\nu h_{11/2}$  or  $\nu d_{5/2}$  neutron behaves as a spectator. This leads to a 3-quasi-particle final state with the  $g_{9/2} \otimes (g_{7/2}, \nu)$  configuration. This mechanism also is likely to apply to the decays of the high-spin odd-odd rhodium isotopes to palladium, where two-neutron quasi-particle states near 2.5 MeV are strongly fed, with  $\log ft$  values of 4.9 [8,31].

Finally, we present the integrated Gamow-Teller strength (GT) for the decay of odd-*A* Ru isotopes in table 4. The value for the  $^{113}\text{Ru}$  low-spin decay is quite comparable to those of other  $5/2^+$  ruthenium decays. However, the GT strength for the decay of the  $^{113}\text{Ru}$  high-spin level is very high. A revision of the Ru spin to  $9/2^-$ , as has been mentioned above as a solution to increase the  $\log ft$  value to the  $9/2^+$  state, would allow sizeable feedings to low-lying  $7/2^+$  states and contribute to decrease the abnormally high  $B(\text{GT})$  value. This, however, seems still to be not enough to get a  $B(\text{GT})$  value in agreement with systematics.

## 4 Conclusion

In this work the decay of  $^{113}\text{Ru}$  isotope to levels in  $^{113}\text{Rh}$  has been studied and the number of transitions has been considerably extended. The low-lying levels observed in  $^{113}\text{Rh}$  confirm previous results. They follow extrapolations of nuclear properties based on a smooth systematical behaviour as a function of mass number. The level structure can be interpreted in the frame of shape coexistence. The lowest-lying levels are spherical and of even parity, showing the importance of seniority  $\nu = 1$  and 3 states built on

the  $g_{9/2}$  proton. The odd parity levels which are expected to go up in energy could not be identified, except for a tentative  $5/2^-$  assignment to the level at 785 keV. The most important new information is confirmation of the  $3/2^+$  level at 601 keV as the band head of the deformed  $K = 1/2$  band. This is supported by the hindrance of its decay to spherical states, which is a systematic feature in Rh isotopes. The  $1/2^+$  level could not be identified. However, the levels at 834 and 786 keV are very reasonable candidates for the next  $5/2^+$  and  $7/2^+$  states, based on their transitions and the parameters deduced from the energy spacings.

Based on spin considerations, separate decay schemes have been constructed for each decay of  $^{113}\text{Ru}$   $5/2^+$  and  $11/2^-$  states. In the high-spin isomer decay we note a too large  $\beta$ -branching to the  $9/2^+$  state ( $\log ft = 5.1$ ) and a large GT strength (0.59), twice the one for the decay of the low spin  $^{113}\text{Ru}$  and of the neighbouring isotopes. A somewhat larger  $\log ft$  value for the transition to the  $9/2^+$  state could be obtained by adding part of the unplaced transitions on top of the  $9/2^+$  level or by a revision of the  $11/2^-$  spin in  $^{113}\text{Ru}$  to  $9/2^-$  resulting in a different sharing of the  $\beta$  feedings. However, these modifications cannot lower the high GT strength by a factor of two.

In conclusion, the new data confirm the features characterizing the structure of odd-mass rhodium isotopes with, in particular, the identification of the  $K = 1/2$  intruder band. This work is part of a more systematical study of this region where elements are refractory and only the ion-guide-based mass separation provides the required intensities for decay studies. We hope that, combined with prompt-fission studies, these systematic investigations will allow to understand this interesting nuclear region.

The lowest-lying levels in  $^{111}\text{Rh}$  and  $^{113}\text{Rh}$  have been interpreted in the spherical framework by analogy with extensive studies of their less neutron-rich isotopes. In contrast, the rotor + particle description was recently proposed for  $^{107,109}\text{Rh}$  by the EUROGRAM collaboration [26]. In that case, the large retardation of the  $E2$  decay out of the  $K = 1/2$  band (the  $3/2^+ \rightarrow 7/2^+$  transition) could be due to  $K$ -hindrance instead of the change of nuclear shape. It is therefore essential to perform very detailed and sensitive measurements, especially of transition rates and moments, in order to establish the nature of the low-lying rhodium levels. Such measurements might be too challenging for some time due to the exotic character of the  $^{113}\text{Ru}$  parent nucleus limiting the production rates. A promising alternative method is the collinear laser spectroscopy of rhodium ground states. The first systematical studies of zirconium isotopes, like rhodium another refractory element, performed with the IGISOL facility in Jyväskylä [33], indeed show that it could be possible.

This work has been supported by the Academy of Finland under the Centre of Excellence Programme 2000-2005 (project No. 44875, Nuclear and Condensed Matter Physics Programme at JYFL). We also wish to thank Dr. M.-G. Porquet for illuminating discussions.

## References

1. J. Kurpeta, A. Płochocki, G. Lhersonneau, J.C. Wang, P. Dendooven, A. Honkanen, M. Huhta, M. Oinonen, H. Penttilä, K. Peräjärvi, J.R. Persson, J. Äystö, contribution to the *2nd International Conference on Exotic Nuclei and Atomic Masses (ENAM 98) 23-27 June 1998, Bellaire, Michigan, USA, AIP Conf. Proc.* Vol. **455** (AIP, New York, 1998) p. 781.
2. J. Kurpeta, G. Lhersonneau, J.C. Wang, P. Dendooven, A. Honkanen, M. Huhta, M. Oinonen, H. Penttilä, K. Peräjärvi, J.R. Persson, A. Płochocki, J. Äystö, *Eur. Phys. J. A* **2**, 241 (1998).
3. J.C. Wang, P. Dendooven, M. Hannawald, A. Honkanen, M. Huhta, A. Jokinen, K.-L. Kratz, G. Lhersonneau, M. Oinonen, H. Penttilä, K. Peräjärvi, B. Pfeiffer, J. Äystö, *Phys. Lett. B* **454**, 1 (1999).
4. H. Penttilä, Ph. D. thesis, University of Jyväskylä (1992).
5. H. Penttilä, P. Dendooven, A. Honkanen, M. Huhta, P.P. Jauho, A. Jokinen, G. Lhersonneau, M. Oinonen, J.-M. Parmonen, K. Peräjärvi, J. Äystö, *Nucl. Instrum. Methods Phys. Res. B* **126**, 213 (1997).
6. P. Dendooven, S. Hankonen, A. Honkanen, M. Huhta, J. Huikari, A. Jokinen, V.S. Kolhinen, G. Lhersonneau, A. Nieminen, M. Oinonen, H. Penttilä, K. Peräjärvi, J.C. Wang, J. Äystö, *Proceedings of the 2nd International Workshop on Nuclear Fission and Fission-Product Spectroscopy, Seyssins, France, 1998*, edited by G. Fioni, H. Faust, S. Oberstedt, F.J. Hamsch, *AIP Conf. Proc.* Vol. **447** (AIP, New York, 1998) p. 135.
7. G. Lhersonneau, B. Pfeiffer, J. Alstad, P. Dendooven, K. Eberhardt, S. Hankonen, I. Klöckl, K.-L. Kratz, A. Nähler, R. Malmbeck, J.P. Omvedt, H. Penttilä, S. Schoedder, G. Skarnemark, N. Trautmann, J. Äystö, *Eur. Phys. J. A* **1**, 285 (1998).
8. G. Lhersonneau, J.C. Wang, S. Hankonen, P. Dendooven, P. Jones, R. Julin, J. Äystö, *Phys. Rev. C* **60**, 014315 (1999).
9. V. Paar, *Nucl. Phys. A* **211**, 29 (1973).
10. N. Kaffrell, P. Hill, J. Rogowski, H. Tetzlaff, N. Trautmann, E. Jacobs, P. de Gelder, D. De Frenne, K. Heyde, G. Skarnemark, J. Alstad, N. Blasi, M.N. Harakeh, W.A. Sterreburg, K. Wolfsberg, *Nucl. Phys. A* **460**, 437 (1986).
11. N. Kaffrell, P. Hill, J. Rogowski, H. Tetzlaff, N. Trautmann, E. Jacobs, P. de Gelder, D. De Frenne, K. Heyde, S. Börjesson, G. Skarnemark, J. Alstad, N. Blasi, M.N. Harakeh, W.A. Sterreburg, K. Wolfsberg, *Nucl. Phys. A* **470**, 141 (1987).
12. J. Rogowski, J. Alstad, M.M. Fowler, D. De Frenne, K. Heyde, E. Jacobs, N. Kaffrell, G. Skarnemark, N. Trautmann, *Z. Phys. A* **337**, 233 (1990).
13. M. Huhta, P. Dendooven, A. Honkanen, G. Lhersonneau, M. Oinonen, H. Penttilä, K. Peräjärvi, V. Rubchenya, J. Äystö, *Nucl. Instrum. Methods Phys. Res. B* **126**, 201 (1997).
14. M. Lahtinen, P.M. Jones, K. Jääskeläinen, K. Loberg, W. Trzaska, *JYFL Annual Report* **11** (1996).
15. J. Kantele, *Handbook of Nuclear Spectrometry* (Academic Press Ltd., 1995).
16. I. Klöckl, B. Pfeiffer, P. Dendooven, H. Gerlicher, A. Honkanen, M. Huhta, P. Jürgens, J. Kurpeta, G. Lhersonneau, M. Oinonen, H. Penttilä, J. Persson, A. Popov, K.-L. Kratz, F. Münnich, J. Äystö, *JYFL Annual Report* **29** (1995).
17. R.B. Firestone, *Table of Isotopes* 8th ed. (John Wiley & Sons, Inc., New York, 1996).
18. W. Urban,  $^{248}\text{Cm}$  fission, private communication, July 1997.
19. J.C. Hardy, L.C. Carraz, B. Jonson, P.G. Hansen, *Phys. Lett.*, B **71**, 307 (1977).
20. G. Lhersonneau, B. Pfeiffer, K.-L. Kratz, T. Enqvist, P.P. Jauho, A. Jokinen, J. Kantele, M. Leino, J.M. Parmonen, H. Penttilä, J. Äystö, *Phys. Rev. C* **49**, 1379 (1994).
21. J. Äystö, P.P. Jauho, Z. Janas, A. Jokinen, J.M. Parmonen, H. Penttilä, P. Taskinen, R. Beraud, R. Duffait, A. Emsallem, J. Meyer, M. Meyer, N. Redon, M.E. Leino, K. Eskola, P. Dendooven, *Nucl. Phys. A* **515**, 365 (1990).
22. G. Lhersonneau, J.C. Wang, S. Hankonen, P. Dendooven, P. Jones, R. Julin, J. Äystö, *et al.*, *Eur. Phys. J. A* **2**, 25 (1998).
23. P. Möller, J.R. Nix, W.D. Myers, W.J. Swiatecki, *At. Data Nucl. Data Tables* **59**, 185 (1995).
24. J. Skalski, S. Mizutori, W. Nazarewicz, *Nucl. Phys. A* **617**, 282 (1997).
25. K. Butler-Moore, R. Aryaeinejad, J.D. Cole, Y. Dardenne, R.G. Greenwood, J.H. Hamilton, A.V. Ramayya, W.-C. Ma, B.R.S. Babu, J.O. Rasmussen, M.A. Stoyer, S.Y. Chu, K.E. Gregorich, M. Mohar, S. Asztalus, S.G. Prussin, K.J. Moody, R.W. Laugheed, J.F. Wild, *Phys. Rev. C* **52**, 1339 (1995).
26. Ts. Venkova, M.-G. Porquet, I. Deloncle, B.J.P. Gall, H. De Witte, P. Petkov, A. Bauchet, T. Kutsarova, E. Gueorgieva, J. Duprat, C. Gautherin, F. Hoellinger, R. Lucas, A. Minkova, N. Schulz, H. Sergolle, E.A. Stefanova, A. Wilson, *Eur. Phys. J. A* **6**, 25 (1998).
27. N. Kaffrell, J. Rogowski, H. Tetzlaff, N. Trautmann, D. De Frenne, K. Heyde, E. Jacobs, G. Skarnemark, J. Alstad, M.N. Harakeh, J.M. Schippers, S.Y. van der Werf, W.R. Daniels, K. Wolfsberg, *Proceedings of the 5th International Conference on Nuclei far from Stability, Rosseau Lake, Ontario, Canada, 1987*, edited by I. Towner (AIP, New York, 1988) p. 286.
28. B. Fogelberg, E. Lund, Y. Zongyuan, B. Ekström, *Proceedings of the 5th International Conference on Nuclei far from Stability, Rosseau Lake, Ontario, Canada, 1987*, edited by I. Towner (AIP, New York, 1988) p. 196.
29. G. Lhersonneau, H. Gabelmann, N. Kaffrell, K.-L. Kratz, B. Pfeiffer, K. Heyde, the ISOLDE Collaboration. *Z. Phys. A* **337**, 143 (1990).
30. H. Mach, B. Fogelberg, M. Sanchez-Vega, A.J. Aas, K.J. Erokhina, K. Gulda, V.I. Isakov, J. Kvasil, G. Lhersonneau, *Proceedings of the International Workshop on Physics of Unstable Beams, Serra Negra, Brazil, 1996*, edited by C.A. Bertulani, L. Felipe Canto, M.S. Hussein (World Scientific, Singapore, 1997) p. 338.
31. J. Äystö, C.N. Davids, J. Hattula, J. Honkanen, K. Honkanen, P. Jauho, R. Julin, S. Juutinen, J. Kumpulainen, T. Lönnroth, A. Pakkanen, A. Passoja, H. Penttilä, P. Taskinen, E. Verho, A. Virtanen, M. Yoshii, *Nucl. Phys. A* **480**, 104 (1988).
32. A. Jokinen, J. Äystö, P. Dendooven, K. Eskola, Z. Janas, P.P. Jauho, M.E. Leino, J.M. Parmonen, H. Penttilä, K. Rykaczewski, P. Taskinen, *Z. Phys. A* **340**, 21 (1991).
33. *JYFL Accelerator News* **9**, August 2001.